Single and double pion production from 800 MeV proton-proton collisions

F. H. Cverna,* P. R. Bevington, M. W. McNaughton,* and H. B. Willard†
Case Western Reserve University, Cleveland, Ohio 44106

N. S. P. King
Los Alamos Scientific Laboratory, Los Alamos, New Mexico 87545

D. R. Giebink
University of Texas, Austin, Texas 78712
and Los Alamos Scientific Laboratory, Los Alamos, New Mexico 87545

(Received 19 June 1980)

The three-body final-state reaction of charged single-pion production, $pp \rightarrow \pi^+ pn$, and that for charged double-pion production, $pp \rightarrow \pi^-\pi^+pp$, have been studied at $T_p = 800$ MeV by measuring the momentum spectra for π^+ and π^- emitted from proton-proton collisions. The momentum spectra for single-pion production are fit with the peripheral model calculations of VerWest, and a similar model by one of us is discussed. The spectra for double-pion production follow an extrapolation of the Lindenbaum and Sternheimer model from higher energies toward threshold. This result is in disagreement with the results of Cochran *et al.*

[NUCLEAR REACTIONS Pion production in the two-nucleon system: $pp \rightarrow \pi^+pn$, $pp \rightarrow \pi^-\pi^+pp$; $E_p = 800$, $\theta = 16.5°-60°$. Observed $d^2\sigma/d\Omega dq_\pi$. Peripheral model analyses.]

I. INTRODUCTION

There has recently been renewed interest in the theoretical and experimental aspects of pion production in nucleon-nucleon collisions at intermediate energies. This paper reports measurements of the pion momentum spectra, i.e., the double-differential production cross sections $d^2\sigma/d\Omega dq$ for the three-body final-state reaction of charged single-pion production, (1) $p+p \rightarrow \pi^+ + p + n$, and for charged double-pion production, (2) $p+p \rightarrow \pi^- + \pi^+ + p + p$, at 800 MeV incident proton energy in the laboratory angular range 16.5° to 60°. Preliminary results have been published elsewhere.[1]

Very little data on reaction (1) near 800 MeV exist other than the work of Cochran *et al.*[2] at 730 MeV and recent measurements accompanying the kinematically complete experiments performed at LAMPF by the Rice-Houston group of Hudomalj-Gabitsch *et al.*[3,4] The data of Cochran *et al.* agree with the one-pion exchange calculation of Suslenko and Kochkin.[5] The measurements reported here have stimulated further calculations that will be described later in this paper.

The measurements of reaction (2), which are only 200 MeV above the threshold for double-pion production, serve to resolve an experimental discrepancy between Cochran *et al.*,[2] who obtained a total cross section of $\sigma = 0.3 \pm 0.1$ mb at 730 MeV and the earlier results of Bugg *et al.*[6] and Barnes *et al.*,[7] who obtained $\sigma = 0.016 \pm 0.02$ mb at 970 MeV. The resolution of this discrepency is important to check the validity of the isobar model and other models near threshold and to determine whether the cross section just above threshold is anomalously large, as it is for neutron-proton collisions.[8]

II. EXPERIMENTAL PROCEDURE

The experimental procedure consisted of observing pion emission from 800 MeV proton-proton collisions. The momentum spectra for π^+ [hence reaction (1)] and π^- [which can only be emitted from the double-pion production reaction (2)] at each angle was determined. The measurements were performed with the external proton beam (EPB) at the Los Alamos Meson Physics Facility (LAMPF) and the magnet spectrometer shown in Fig. 1. The spectrometer consisted of three (X-Y) pairs of multiwire proportional chambers[9] (MWPC's) ($M1$, $M2$, and $M3$), which provided trajectory information,[10] and a "C" magnet (18D40) for momentum separation. Two scintillators ($S1$ and $S2$) provided timing information, while the gas Čerenkov detector (C) identified electrons. A fourth pair of MWPC's ($M4$) served to identify two-body final states and was typically set to tag proton-proton elastic scattering events. The target was liquid hydrogen of density 0.0708 gm/cm^3. The target vessel was made of 0.127 mm kapton with additional wrappings of 0.25 mil aluminized Mylar for thermal stability.

The magnetic spectrometer was designed to maximize the acceptance of the expected π^- momentum distribution for determination of double-pion production. The spectrometer's acceptance is shown in Fig. 2. The telescope of MWPC's

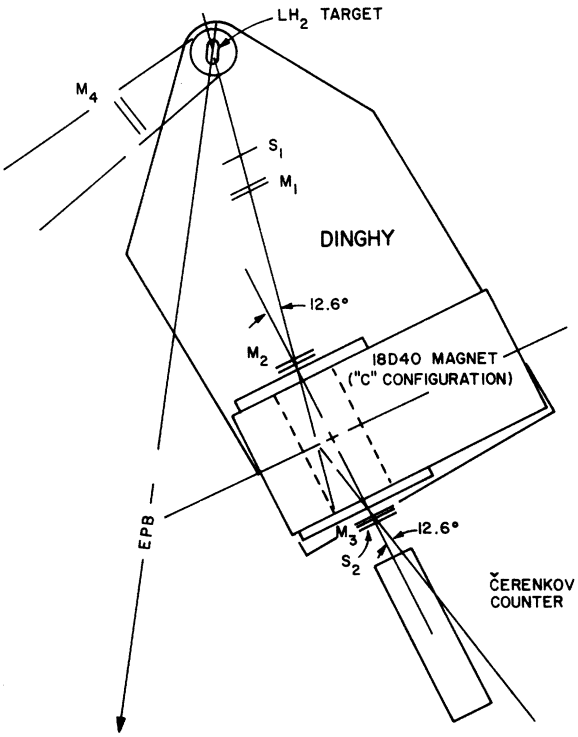

FIG. 1. Scale drawing of experimental apparatus.

($M1$ and $M2$) rejected particles emitted from outside the central 5 cm of the 6.5 cm thick LH_2 target (e.g., from the target end walls). Runs were made with the target full and empty to provide further subtraction of background. The beam intensity was monitored relatively with an ion chamber. This method was most reliable at low beam currents. At high beam currents, the ion chamber was normalized absolutely with a Faraday cup.[11]

The data were corrected for several effects. As is shown in Fig. 2, particles emitted from the target and traversing MWPC's $M1$ and $M2$ had a 100% acceptance by the spectrometer into $M3$ in the momentum range of 115 to 275 MeV/c for a magnet current of 100 A. The momentum range scaled with magnet current. Particles detected in the nonuniform acceptance regions at the low and high ends were weighted by their inverse probability of acceptance. A correction for the decay of pions in flight, which combined the known lifetime of the pion, the length of the pion's flight path, and the pion's momentum, was made for each pion trajectory.

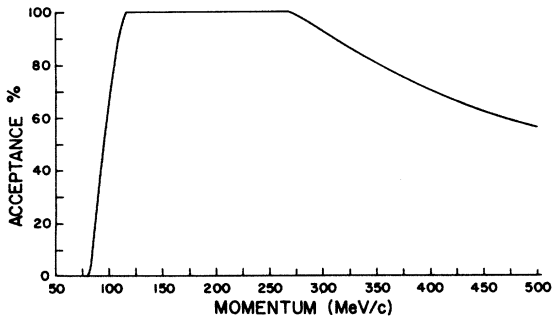

FIG. 2. Spectrometer acceptance vs momentum at 30° and 100 A magnet current.

The largest correction was made to the measured dead time. Since dead time was determined with a real-time clock instead of with a beam-related monitor, any fluctuations in beam intensity resulted in erroneous measurements of dead time. During the experiment it was believed that a nearly constant beam intensity was typical in EPB. That beam is now known to have a discontinuous structure on the macropulse (500 μs) level, as well as sinusoidal variations in intensity (by a factor of 2 at a frequency of about 10 Hz.[12]

Comparison of the measured differential cross section for elastic proton-proton scattering with published cross sections[13] indicated that the measured dead time was about half that needed to give reasonable agreement. The known variations in the EPB can fully account for this discrepancy. Thus, based on the measurements of proton-proton elastic scattering, a correction factor of 2 was applied to the measured dead time, which improved the agreement to within 10%. This correction necessitates the assigning of a 10% systematic uncertainty to the pion-production data at each angle and magnet current. It should be noted that all later experiments by this group (e.g., measurements of A_y, Ref. 14) based measurements of dead time on a beam-related monitor.

III. SINGLE PION PRODUCTION

The laboratory momentum spectrum for observed π^+ from reaction (1) are shown in Fig. 3. The error bars shown are statistical only and do not include the 10% systematic uncertainty from dead time. Spectra taken with different magnet currents have been combined. The spectra exhibit peaking similar to that seen in the kinematically complete data of Ref. 3 and 4. The peak position in the π^+ momentum spectra is approximately that calculated by considering the decay of a stationary Δ^{++} in the over-all-center-of-mass (OACM) reference frame.

A study of the pion-production mechanism is best carried out in the OACM where symmetry about $\theta_{c.m.} = 90°$ permits parametrization of the data in even powers of $\cos\theta_{c.m.}$. This facilitates

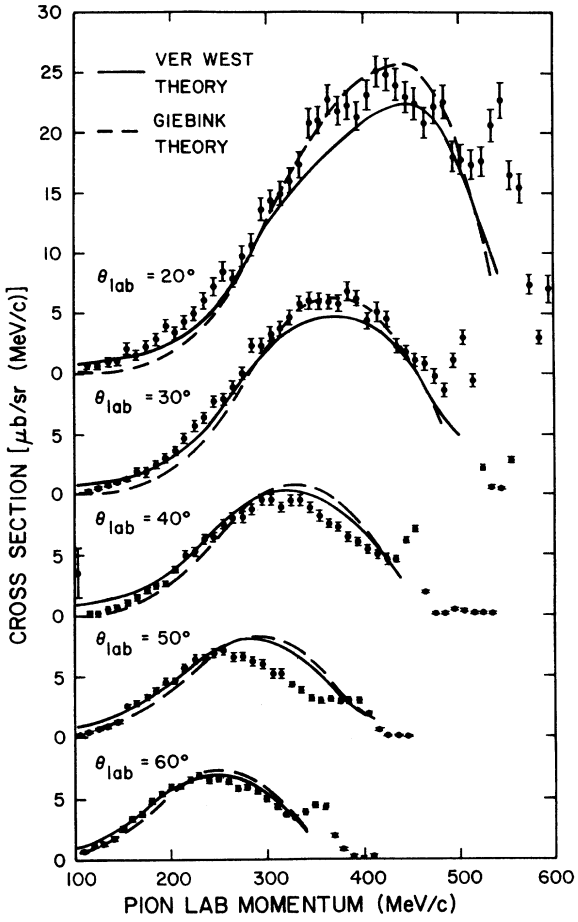

FIG. 3. Momentum spectra of π^+ (laboratory reference frame).

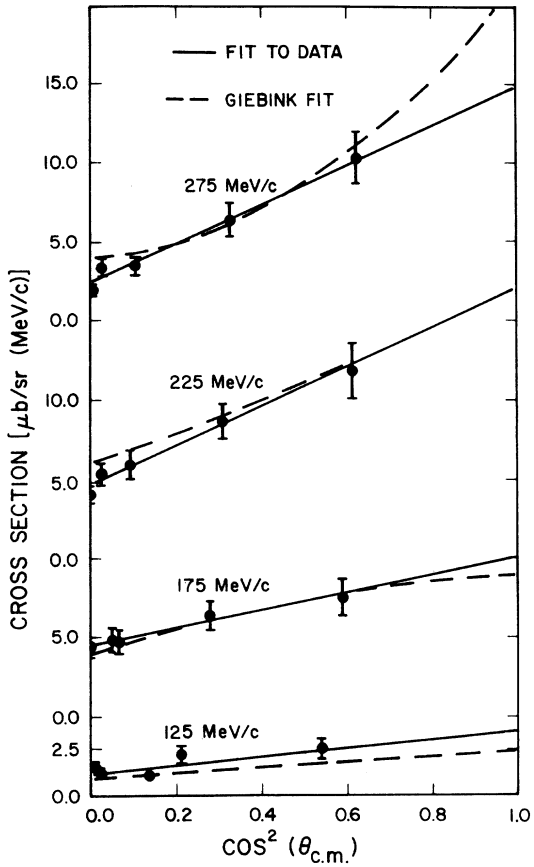

FIG. 4. Angular distributions of π^+ at selected over-all-center-of-mass (OACM) momenta of 125, 175, 225, and 275 MeV/c. Solid lines are least-squares fits to the data. Dashed lines are from the calculations of Giebink (α =730 MeV/c).

a meaningful comparison with other data and theoretical predictions.

The data have been parametrized with Legendre polynomials

$$\frac{d^2\sigma}{d\Omega dq} = c_0 P_0 + c_2 P_2(\cos\theta_{c.m.}) + \cdots + c_i P_i(\cos\theta_{c.m.}),$$

(i is even and q is the pion momentum in the OACM), which are orthogonal over the angular range, rather than with the historical form of a power series in $\cos^2\theta_{c.m.}$. The orthogonality assures that the value of low-order terms (e.g., c_0 and c_2) are minimally dependent on whether or not those for higher-order terms (e.g., c_4) can be extracted.

Figure 4 shows the angular distribution for the present data in the OACM at several values of the pion momentum. The error bars shown include the 10% systematic uncertainty for dead time. The solid lines are least-squares fits to the data to order $P_2(\cos\theta_{c.m.})$. Fits to order $P_4(\cos\theta_{c.m.})$ were excluded by a χ^2 analysis. The lack of curvature (P_4 term) in the fits can be attributed to a lack of data at $\cos^2\theta_{c.m.} \cong 1$. The integrated center-of-mass cross section $d\sigma/dq = 8\pi^2 c_0$ is shown in Fig. 5. The ratio c_2/c_0, which is independent of the data normalization, is shown in Fig. 6.

Essentially two methods are used for the theoretical analysis of reaction (1). The first method is the one-meson-exchange (or peripheral) model, which has been used extensively in the past for studying the reactions $NN \to NN\pi$ (Refs. 4, 5, 15–18) and $pp \to d\pi^+$.[19] At 800 MeV, this model is simplified for reaction (1) by the fact that the initial-state pp interaction is negligible and the final-state pn interaction is expected to be small over much of the pion-momentum range. Two calculations of this type will be discussed below. The second method is to solve a complete set of relativistic, three-body equations for the $NN\pi$ system.[20] Calculations of this type will not be discussed here.

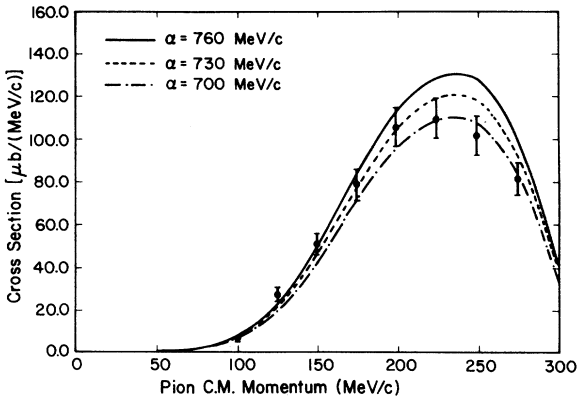

FIG. 5. Cross section for π^+ production integrated over angle ($d\sigma/dq = 8\pi^2 c_0$). Lines are from the calculation of Giebink using different form factors. Solid line, $\alpha = 760$ MeV/c. Dashed line, $\alpha = 730$ MeV/c. Dot-dash line, $\alpha = 700$ MeV/c.

VerWest[17] has recently completed a calculation within the peripheral-model framework. Field-theoretic methods were used to incorporate π and ρ exchange. The πN-πN and ρN-πN off-mass-shell scattering amplitudes were generated via the exchange of N and Δ isobars. Coupling constants and form factors were adjusted to obtain a best fit to on-shell πN scattering data and the pion-production cross section [reaction (1)]. The results of this calculation are shown in Fig. 3.

One of us (D.R.G.) has performed a peripheral-model calculation for reaction (1),[18] which is more phenomenological than that of VerWest. In this calculation, the on-shell πN scattering amplitude,[21] modified by a form factor in the relative πN momentum, is used for the off-energy-shell πN-πN scattering vertex. Only pion exchange is considered and the emission vertex is given by the field-theoretic, pseudoscalar interaction Hamiltonian. Relativistic effects are included through the use of Wick's three-body formalism.[22] This formalism allows one to study the effect of form-factor variations, to investigate the importance of the small πN partial-wave scattering amplitudes, and to begin a formal study of the driving term in a relativistic three-body theory. In this context, reaction (1) provides an ideal testing ground for many of the approximations that are currently employed in pion-nuclear scattering theories.

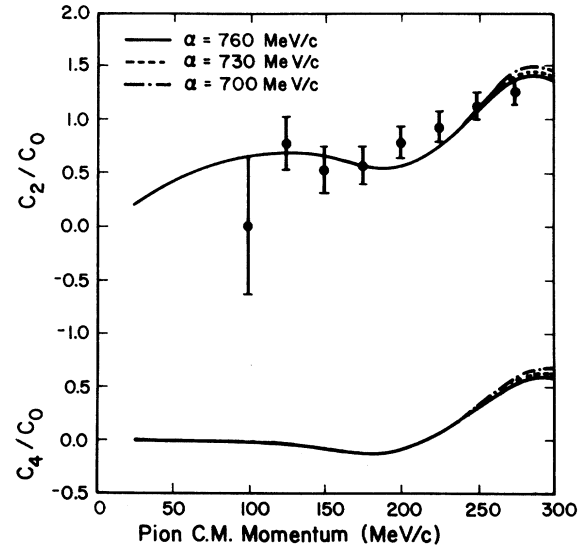

FIG. 6. Ratio of the coefficients c_i/c_0 for the Legendre polynomial fits to the differential cross section. Lines are as in Fig. 5.

Figures 3–6 show our fit to the present data. Form factors in the relative πN momentum, $\nu(p) = \exp(-p^2/\alpha^2)$, were included on the P-wave parts of the scattering vertex and on the emission vertex. The best fit was obtained with $\alpha = 730$ MeV/c. This value is in reasonable agreement with a Chew-Low determination of the πN form factor by Ernst and Johnson.[23] These figures indicate that the primary function of the form factor is to adjust the magnitude of the integrated cross section $d\sigma/dq$. The angular distribution is insensitive to form factor variations.

We have also considered the pion asymmetry in the reaction $p+p \to \pi^+ + p + n$. The cross section for observed π^+ is again parametrized in Legendre polynomials

$$\frac{d^2\sigma}{d\Omega dq}_{\text{polarized}} = \frac{d^2\sigma}{d\Omega dq}_{\text{unpolarized}} + \vec{\Pi}\cdot\hat{n}\sin\theta_{\text{c.m.}}[d_0 + P_0 + d_1 P_1(\cos\theta_{\text{c.m.}}) + \cdots + d_i P_i(\cos\theta_{\text{c.m.}})] .$$

($\vec{\Pi}$ is the beam-polarization vector and $\hat{n}$ is the beam direction.) Figure 7 shows the effect of form factor variations on the ratios d_i/c_0. These ratios are also insensitive to form-factor variations.

One of the approximations that is often used in pion-nuclear calculations is the assumed dominance of the P_{33} pion-nucleon partial wave in the Δ^{++} resonance region. Figures 8–10 show the effect of keeping only the P_{33} partial wave at the πN-πN scattering vertex. The integrated cross section and the unpolarized angular distribution are insensitive to this assumption. However, the asymmetry shows a strong sensitivity to the "small" S- and P- pion-nucleon partial waves, which are often neglected or poorly fit. The theory of VerWest,[17] for example, can fit the P_{11} and P_{33} on-shell πN partial waves, but it cannot accurately fit the other partial wave amplitudes.

A more complete theoretical investigation of

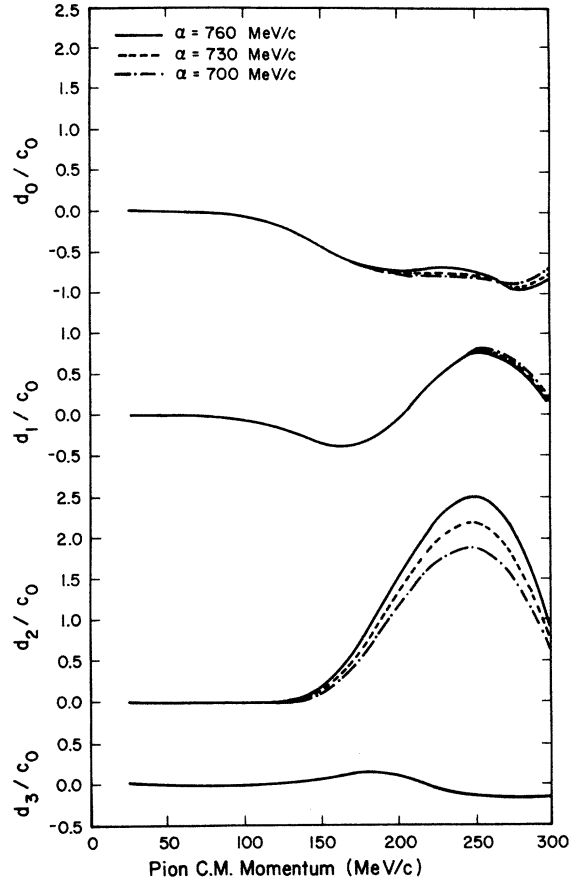

FIG. 7. Ratio of the coefficients d_i/c_0 for the Legendre polynomial fit to the asymmetry. Lines are as in Fig. 5.

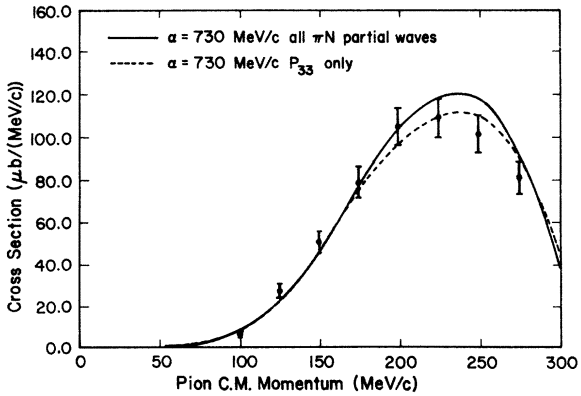

FIG. 8. Cross section for π^+ production integrated over angle. Lines are from the calculation of Giebink (α =730 MeV/c). Solid line includes all S- and P-partial wave amplitudes at the $\pi N \to \pi N$ scattering vertex. Dashed line includes only the P_{33} partial wave amplitude at this vertex.

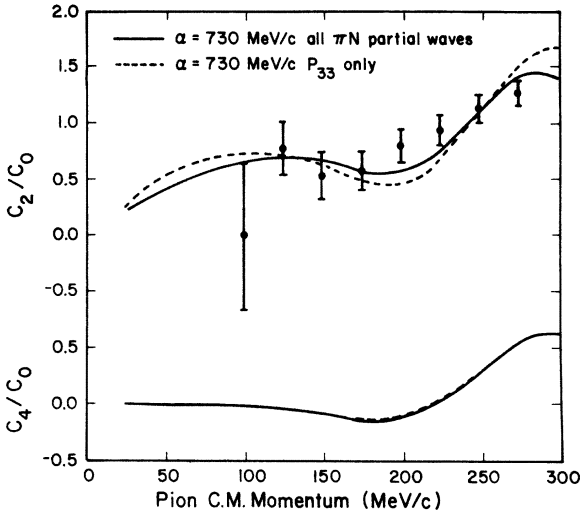

FIG. 9. Ratio of the coefficients c_i/c_0 for the Legendre polynomial fits to the differential cross section. Lines are as in Fig. 8.

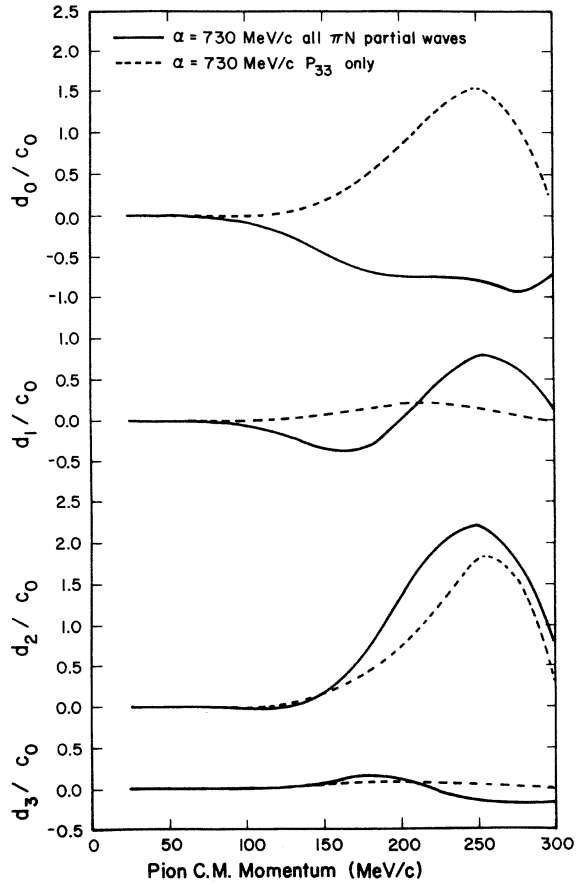

FIG. 10. Ratio of the coefficients d_i/c_0 for the Legendre polynomial fits to the asymmetry. Lines are as in Fig. 8.

this reaction is in progress and will be reported elsewhere.

IV. DOUBLE PION PRODUCTION

The observed momentum spectra of the π^- in the laboratory system are shown in Fig. 11. The error bars on the data (binned in 20 MeV/c intervals) represent the statistical uncertainties. The appearance of accidentals at momenta above the kinematic limit is quite apparent. These accidentals are especially prevalent at back angles (e.g., 60° where the kinematic limit is less than 200 MeV/c) and are probably due to protons scattered inelastically from the target. This conjecture will be discussed later in this section.

The production of μ^- from the decay of π^- in flight and electrons from the target contributed to background contamination. The μ^- were rejected by trajectory analysis in the vertical direction. The number of electrons from the target was about three times the number of π^-. These electrons were identified by time of flight (TOF) and the gas Čerenkov detector. The resolution of the TOF spectra was not sufficient to discriminate between pions with momentum greater than 125 MeV/c ($\beta \gtrsim 0.7c$) and electrons ($\beta \simeq 1$). Therefore, TOF rejection criteria was only applied to low momentum particles. The efficiency of the Čerenkov detector was determined by comparing the cut on the data imposed by the TOF measurement to that imposed by the Čerenkov detector at low momenta. This comparison indicated that the Čerenkov counter effectively eliminated the electron contamination.

The theory of double-pion production at this energy is quite crude. The isobar model of Lindenbaum and Sternheimer[24] is one of the few calculations that has been performed. They assume that production occurs via one or both of the following reactions:

$$N+N \rightarrow N^* + N^* \qquad N+N \rightarrow N^* + N$$
$$\downarrow \quad \downarrow \qquad\qquad \downarrow$$
$$N+\pi \quad N+\pi, \qquad\qquad N+\pi+\pi.$$

This close to threshold, however, the predicted angular distributions are indistiguishable from those of pure phase-space calculations.

The momentum distributions for the π^- transformed to the over-all-center-of-mass (OACM) are shown in Fig. 12. Also shown in Fig. 12 are the results of a statistical three-body-phase-space calculation that is based on the Block formalism.[25] The three phase-space curves shown are normalized to integrated cross sections of 2, 3, and 4 μb, respectively.

There is considerable disagreement between the

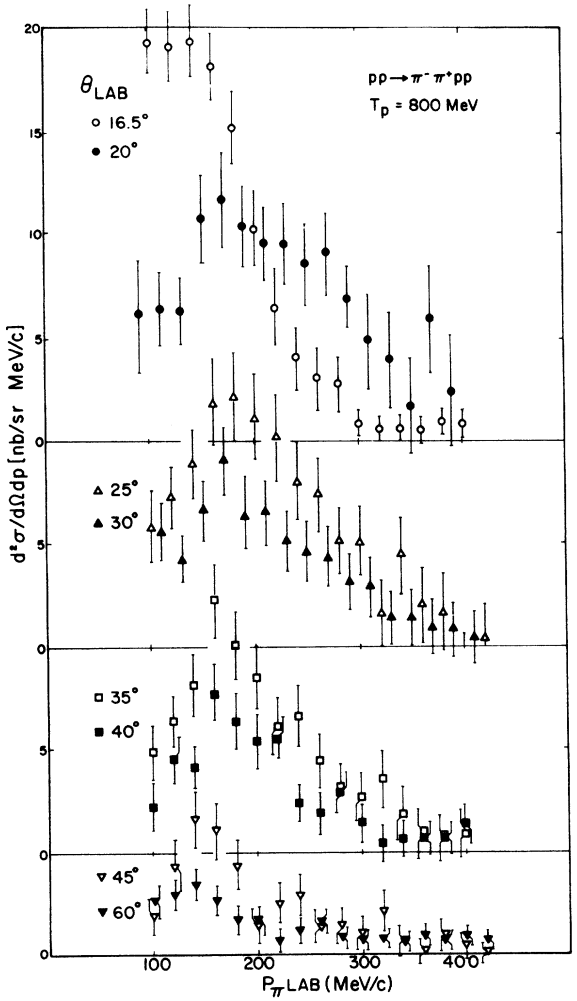

FIG. 11. Momentum spectra of π^- (laboratory reference frame).

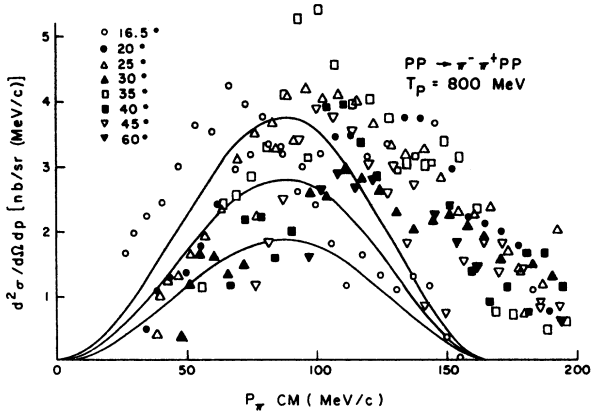

FIG. 12. Momentum spectra (OACM) for $pp \rightarrow \pi^-\pi^+pp$. Solid lines are phase-space calculations (Ref. 25).

shapes of the phase-space curves and the measured spectra. There is an excess of measured particles in the high-momentum region and in the nonphysical region above the kinematic limit. One source of contamination in this region has already been rejected, after identification by the conjugate detector $M4$, as being correlated with elastically scattered protons. If an equal yield of the same shape is subtracted once more, assuming that there should be a similar contamination correlated with inelastically scattered protons from single-pion production, the yield in the nonphysical region nearly vanishes. The yield below the kinematic limit is then approximately a symmetrical shape about 80 MeV/c. This shape is characteristic of the phase-space curves.

Contributions from electrons are expected to be largest in the low momentum region. However, the rejection of electrons by TOF and the Čerenkov detector should be adequate at all angles except 16.5°. At this angle there are relatively more high momentum particles, and the position of the Čerenkov detector was biased to ensure their rejection. Some particles with laboratory momentum in the range 100 to 200 MeV/c then had trajectories that missed the Čerenkov detector. Unfortunately, TOF analysis was not adequate to reject the remaining electrons in this region. Thus the low momentum 16.5° data are probably not reliable.

With emphasis on the region below 100 MeV/c (Fig. 12), one can see that the measured yields at the various center-of-mass angles are the same. This supports our identification of the particles as pions. Then, since the observed cross sections fall roughly between the limits of the solid curves representing 2 and 4 μb, we take the integrated cross section to be 3 ± 1 μb.

The excitation function for reaction (2) is shown in Fig. 13. The solid curve is adapted from Ref. 24. The data presented here are in good agreement with the extrapolation of the solid curve to low energies. The point at 730 MeV is the work of Cochran *et al.* These data were measured using a scintillator hodoscope, which probably overestimated the yield because of background contamination. The points at 970 MeV are those of Bugg *et al.*[6] and Barnes *et al.*[7] and represent the detection of only one event in a bubble chamber. References for higher energy data are given in Ref. 1.

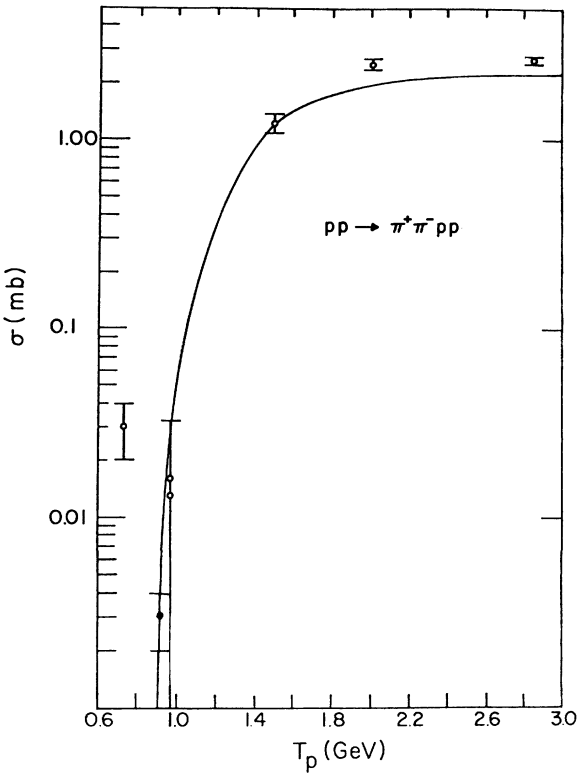

FIG. 13. Total cross section for double-pion production in proton-proton collisions vs incident proton energy (laboratory reference frame). Solid line is an extrapolation from the calculation of Lindenbaum and Sternheimer (Ref. 24).

V. CONCLUSIONS

Knowledge of the πN interaction in a many-body environment is a necessary input to many theoretical models in medium-energy physics. The two-nucleon system is the simplest many-body system that can be used to investigate this interaction. The reaction $pp \to \pi^+ pn$ at 800 MeV is especially simple, because it can be adequately described by single-meson-exchange theories. The data presented here, together with kinematically complete data,[3,4] provide a reasonable set of experimental results for this reaction; yet, from a theoretical viewpoint these data are incomplete.

It was shown that the unpolarized differential cross section could be well fit with the theory of VerWest,[17] which is field theoretic and includes both π and ρ exchange in the peripheral model. But the data were equally well fit with a theory that included only π exchange, and the unpolarized cross section was found to be insensitive to the exact form of the πN-πN scattering vertex. The asymmetry, on the other hand, is sensitive to these theoretical manipulations. Thus it appears that kinematically complete asymmetry measurements, such as those performed by the Rice-Houston-LASL-CWRU collaboration,[26] will be useful in improving the theoretical understanding of this reaction and other reactions of this type. We also believe that good statistics in inclusive differential cross section and asymmetry measure-

ments (i.e., single-arm experiments) would be of equal value.

The experiment on double-pion production was originally designed to measure π^- cross sections on the order of 1 μb/sr (MeV/c). Despite the fact that the experimentally measured cross section turned out to be 100 times lower, we were able to show that the angular distributions were consistent with predictions. The data presented here tend to confirm the validity of an isobar model near threshold. The calculated cross section indicates that there is no anomalously high double-pion production near theshold, as the data of Cochran *et al.* had indicated. Until a more sensitive theoretical model is available, the data presented here seem to be an adequate experimental base for double-pion production at 800 MeV.

ACKNOWLEDGMENTS

The authors are deeply indebted to B. J. VerWest for fitting the data presented here with his calculation, and to E. R. Winkelmann for helpful discussions of the data reduction and analysis. We also wish to thank H. W. Baer, who helped in the running of this experiment, and the LAMPF staff for their assistance in setting up the equipment and providing a high quality operation of the accelerator. This work was supported in part by the U.S. Department of Energy and Associated Western Universities.

---

*Present address: Los Alamos Scientific Laboratory, Los Alamos, New Mexico 87545.

†Present address: National Science Foundation, Washington, D. C. 20550.

[1]P. R. Bevington, in *Proceedings of the Second International Conference on Nucleon-Nucleon Interactions—1977, Vancouver*, edited by H. Fearing, D. Measday, and A. Strathdee (AIP, New York, 1978), p. 315.

[2]D. R. F. Cochran *et al.*, Phys. Rev. D 6, 3085 (1972).

[3]J. Hudomalj-Gabitsch *et al.*, Phys. Lett. 60B, 215 (1976); J. Hudomalj-Gabitsch *et al.*, in *Proceedings of the Second International Conference on Nucleon-Nucleon Interactions—1977, Vancouver*, edited by H. Fearing, D. Measday, and A. Strathdee (AIP, New York, 1978), p. 551.

[4]J. Hudomalj-Gabitsch *et al.*, Phys. Rev. C 18, 2666 (1978).

[5]V. C. Suslenko and V. I. Kochkin, JINR Report No. P2-5572, 1971 (unpublished).

[6]D. V. Bugg *et al.*, Phys. Rev. 133, B1017 (1964).

[7]V. E. Barnes *et al.*, Phys. Rev. Lett. 7, 288 (1961).

[8]W. O. Lock and D. F. Measday, *Intermediate Energy Nuclear Physics* (Meuthen, London, 1970).

[9]P. R. Bevington *et al.*, Nucl. Instrum. Methods 129, 373 (1975).

[10]P. R. Bevington and R. A. Leskovec, Nucl. Instrum Methods 147, 431 (1977).

[11]R. J. Barrett *et al.*, Nucl. Instrum Methods 129, 441 (1975).

[12]O. B. Van Dyck, LAMPF (private communication).

[13]H. B. Willard *et al.*, Phys. Rev. C 14, 1545 (1976).

[14]P. R. Bevington *et al.*, Phys. Rev. Lett. 41, 384 (1978).

[15]E. Ferrari and F. Selleri, Nuovo Cimento Suppl. 24, 453 (1962).

[16]E. Borie, D. Dreschel, and H. J. Weber, Z. Phys. 267, 393 (1974); F. Selleri, Nuovo Cimento 40A, 236 (1965).

[17]B. J. VerWest, Phys. Lett. 83B, 161 (1979).

[18]D. R. Giebink, W. R. Gibbs, and E. R. Siciliano in *Meson-Nuclear Physics—1979, Houston*, Proceedings of the 2nd International Topical Conference on Meson-Nuclear Physics, edited by E. V. Hungerford III (AIP, New York, 1979). (A more detailed account of this theoretical model is in preparation.)

[19]J. Chai and D. O. Riska, Michigan State University Report No. 1979/203-3, and references therein.

[20]W. M. Kloet and R. R. Silbar, LASL Report No. LA-UR-79-2138, and references therein (unpublished).

[21]G. Rowe, M. Salomon, and R. Landau, Phys. Rev. C 18, 584 (1979).

[22]G. C. Wick, Ann. Phys. (N. Y.) 18, 65 (1962).

[23]D. J. Ernst and M. B. Johnson, Phys. Rev. C 17, 247 (1978).

[24]S. J. Lindenbaum and R. M. Sternheimer, Phys. Rev. 105, 1874 (1957); R. M. Sternheimer and S. J. Lindenbaum, *ibid.* 123, 333 (1961).

[25]M. M. Block, Phys. Rev. 101, 796 (1976).

[26]G. S. Mutchler and P. R. Bevington, LAMPF Progress Report No. LA-8293-PR, 36 (unpublished).